Fuel/Module Impact Load in a Submerged Fuel Storage

H. Durlofsky

Structural Mechanics Associates,
1183 Bordeaux Drive, Suite 13, Sunnyvale, California 94086, U.S.A.

P.C. Sun

Nuclear Fuel & Services Division, General Electric Company,
175 Curtner Avenue, San Jose, California 95125, U.S.A.

SUMMARY

Effects of impacts between fuel bundles and storage tubes on the internal forces in high density fuel racks under seismic loading is examined for both fixed and sliding base fuel storage racks. Hydrodynamic effects due to fluid within the tubes are included in this study. Results indicate that impact and hydrodynamic effects tend to reduce the internal forces in fuel racks where base sliding is permitted, while these effects increase internal forces in fixed base fuel racks. In fixed base racks the magnitude of the increase in internal forces is shown to be highly dependent on the fuel-structure mass ratio.

1. Introduction

High density fuel storage modules have been increasingly utilized at reactor sites for the purpose of storing discharged spent fuel. The module usually has a honeycomb construction with a rectangular cross section as shown in Figure 1. Each cell in the module provides space for a single fuel bundle. The fuel is stored in the vertical position with the entire module submerged in the pool. Modules with sliding supports are used in order to reduce dynamic disturbance due to seismic floor motion.

Fuel bundles in the storage module are not laterally restrained and hence are free to vibrate within the storage tubes due to seismic disturbance. Under the seismic loading, the fuel will frequently impact the storage tube and these impacts can significantly effect the overall response of the storage module. Further, the hydrodynamic behavior of the fluid within the tube can have a significant effect on the magnitude of these impacts.

This paper presents a method for evaluating the fuel bundle and tube impact effects, including the hydrodynamic effects of the fluid within the tubes. The method presented is a dynamic, direct stiffness procedure (1) in which the basic components of the fuel storage modules are characterized as individual spring-mass elements with associated stiffness and mass matrices. These element stiffness and mass matrices are derived by means of Rayleigh functions (2), and are combined into a global system. A direct, time-integration procedure is applied to obtain solutions to the resulting equations of motion.

2. Element Mass and Stiffness Matrices

The behavior of the fuel storage module, shown in Figure 1, under seismic excitation can be evaluated by considering a single fuel bundle and encasing tube shown in Figure 2. The system of Figure 2 is idealized into the mathematical model shown in Figure 3, which consists of four elements. The first element is composed of mass points 1 and 2 and spring k_1, and is used to characterize the behavior of the encasing tube shown in Figure 2. The second element is composed of nodes 1 and 3 and is used to characterize the behavior of the fuel bundle shown in Figure 2. The third element is composed of nodes 2 and 3 and is used to characterize the hydrodynamic effects of the fluid between the encasing tube and the fuel bundle. The fourth and last element consists of nodes 1 and 4, and the elastic-perfectly plastic spring k_2, and is used to characterize the friction connection between the module base and the building floor. The spring constants and mass values associated with the model of Figure 3 are developed by a Raleigh-Ritz procedure.

The encasing tube shown in Figure 2 is considered to behave as a cantilevered beam, and the deflected shape is assumed to be given by

$$u = u_1 + (u_2 - u_1)\left(1 - \cos\frac{\pi x}{L}\right) \tag{1}$$

where u_1 and u_2 are the displacements assoicated nodes 1 and 2 of Figure 3, L is the length of the encasing tube and x is the coordinate along the length. The stiffness matrix associated with the element 1 can be developed from the strain energy functional in the usual manner, with the strain energy functional and elements of the stiffness matrix given by

$$U = \frac{EI}{2}\int_0^L \left(\frac{\partial^2 u}{\partial x^2}\right)^2 dx \tag{2}$$

$$k_{ij} = \frac{\delta^2 U}{\delta u_i \, \delta u_j} \tag{3}$$

Application of equations 1, 2 and 3 gives the following expression for the stiffness matrix associated with element 1 of Figure 3.

$$K_e = \frac{\pi^2 EI}{32 L^2}\begin{bmatrix} 1 & -1 \\ -1 & 1 \end{bmatrix} \tag{4}$$

where EI is the lateral bending stiffness of the tube of Figure 2.

The mass matrix associated with element 1 of Figure 3 develops from the expression for the kinetic energy in the usual manner

$$T = \frac{\rho}{2}\int_0^L (\dot{u})^2 dx \tag{5}$$

$$m_{ij} = \frac{\delta^2 T}{\delta \dot{u}_i \, \delta \dot{u}_j} \tag{6}$$

where ρ represents the mass per unit length. Application of equations 1, 5 and 6 then gives

$$M_e = \rho L \begin{bmatrix} \frac{1}{2} & \frac{4-\pi}{2\pi} \\ \frac{4-\pi}{2\pi} & \frac{3\pi-8}{2\pi} \end{bmatrix} \tag{7}$$

It should be noted that expressions similar to equations 4 and 7 can be obtained by use of generalized spring and mass values obtained from a finite element, modal analysis of the fuel rack structure. The displacement function for the fuel bundle shown in Figure 2 and represented by element 2 of Figure 3 is assumed given by

$$u = u_1 + (u_2 - u_1)\frac{x}{L} \tag{8}$$

application of equations (5) and (6) then gives

$$M_e = \rho L \begin{bmatrix} 1/3 & 2/3 \\ 2/3 & 1/3 \end{bmatrix} \tag{9}$$

The hydrodynamic effects of the fluid between the fuel bundles and encasing tubes can be approximated by postulating a velocity field expressed in terms of the nodal displacements u_2 and u_3 , and determining the kinetic energy associated with this velocity field. Equation (6) is then applied to determine the element mass matrix associated with the fluid. The details of this development are lengthy and will not be given here, but are presented in Reference 3. Finally, the element stiffness matrix associated with element 4 of Figure 3 is given by the usual formulation for a simple spring.

3. Method of Analysis

The element stiffness and mass matrices described in section 2 are assembled into a global system representing the equations of motion for the model shown in Figure 3. A numerical time-integration scheme is applied to these assembled equations of motion. Due to the non-linearities in this system, the element matrices and global equations are reformulated at each time step. Nodes 2 and 3 of Figure 3 are tested for impact after each time step, and when an impact occurs, a central impact formulation is applied to determine separation velocities. These separation velocities are applied as initial conditions for the next time step. In cases where the module is considered to be fixed at the base, node 1 of Figure 3 is fixed and seismic accelerations are applied to nodes 2 and 3. For analyses where sliding is included, the yield force in the elastic-perfectly plastic spring, k_2 of Figure 3, is assigned a value associated with the friction between the module base and the building floor. In addition, for sliding analyses the mass point representing the building structure, node 4 of Figure 3, is assigned a very large value and seismic accelerations are applied only to this node.

The effects of fluid hydrodynamic mass and impacts between fuel bundles and encasing tubes is evaluated by performing similar analyses on the models of Figures 3 and 4. The model of Figure 3 includes both impact and hydrodynamic effects. In the model of Figure 4 impact and hydrodynamic effects are precluded by lumping the mass of the fuel bundles to the encasing tubes, the procedure usually applied in stress analyses of the fuel module assembly. Hydrodynamic and impact effects are then evaluated by subjecting the models of Figures 3 and 4 to the same seismic base accelerations, and monitoring the spring loads, k_1. This procedure is applied to both sliding and fixed base analyses. Choice of a suitable time increment for the numerical integration procedure was determined by reducing the integration time step until no significant changes in the results were evident.

4. Description and Results of Analyses

Two sets of analyses were performed on the models of Figures 3 and 4: one set in which base slide was permitted, and the second set in which the models were fixed at the base (node 1). For the sliding cases, analyses corresponding to three different coefficients of friction between the module and building floor base were performed. The three coefficients considered are 0.132, 0.2, and an infinite coefficient (or fixed base). In these analyses, the gapped and lumped models (shown in Figures 3 and 4 respectively) were subjected to identical seismic base accelerations, and the maximum load in the spring k_1 was monitored. The results of the sliding analyses are presented in Table 1. The second set of analyses was performed to evaluate the effect of the ratio of the fuel mass to the structural mass for fixed base modules. Again, the maximum spring load in spring k_1 was monitored in each analysis. The results of these analyses are presented in Table 2.

5. Discussion of Results and Concluding Remarks

In the models used in this study the gapped model includes the nonlinear hydrodynamic and impact effects, while the lumped model precludes these effects in a manner consistent with usual industry practice. As a result, a comparison of results from the gapped and lumped models of Figures 3 and 4, respectively, provides a measure of the nonlinear hydrodynamic mass and impact effects presently excluded from most stress analyses of high density fuel modules.

Table I presents results from the sliding analyses. In this table, the ratio of the maximum forces monitored in springs k_1 of Figures 3 and 4 are given for two values of base friction and for a fixed base case. From this table it can be seen that when sliding is permitted, the maximum load monitored in the gapped model is less than the corresponding load in the lumped model. This indicates that the nonlinear effects included in the gapped model reduce the spring load. However, for the fixed base case this situation is reversed and the nonlinear effects increase the spring load.

Table II presents results from fixed base analyses. In Table II, the ratio of the maximum spring load in the lumped model to the maximum spring load in the gapped model is given for three different ratios of fuel to structure mass. All of these results indicate larger forces in the gapped model. These results further indicate that the gap effects are most severe in structures having large fuel to structure mass ratios. Hydrodynamic effects due to fluid in the pool outside of the fuel storage modules are usually included in the analysis as a virtual mass lumped to the structural mass of the module (4). This virtual mass can be many times greater than the structural mass, and hence has a significant effect on the predicted nonlinear behavior of the fixed base modules.

6. Reference

(1) Bathe K. J., Wilson, E. L., Numerical Methods in Finite Element Analysis, Prentice-Hall Inc., New Jersey, 1976.

(2) Clough, R. W., Penzien, J., Dynamics of Structures, McGraw-Hill Book Company, New York, 1975.

(3) Durlofsky, H., Analysis of Effects of Gaps on the Dynamic Response of Fuel Assemblies During a Seismic Event, Structural Mechanics Analysis Report Number 77-3, April 1977.

(4) Fritz, R. J., "The Effect of Liquids on the Dynamic Motions of Immersed Solids", ASME Journal of Engineering for Industry, 1972, pp 167.

Table I Relative Spring Forces in Lumped and Gapped Models for Sliding Analyses

Friction Coefficient	Maximum Force in Gapped Model / Maximum Force in Lumped Model
0.132	0.647
0.200	0.493
∞	1.514

Table II Relative Spring Forces in Lumped and Gapped Models for Fixed Based Analyses

Fuel Mass / Structural Mass	Maximum Force in Gapped Model / Maximum Force in Lumped Model
0.8333	1.35
1.43	1.71
5.0	2.05

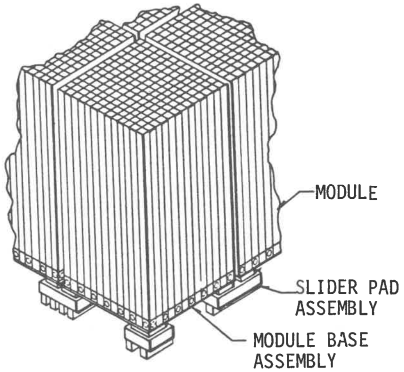

Figure 1 High Density Fuel Storage Module

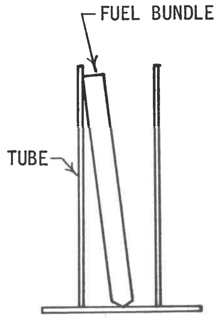

Figure 2 Characterization of Module as a Single Tube and Fuel Bundle

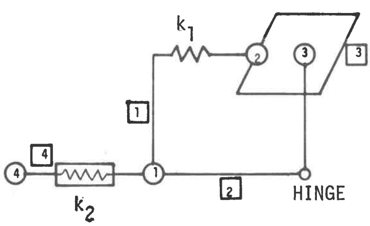

Figure 3 Gapped Element Model of Fuel Storage Module

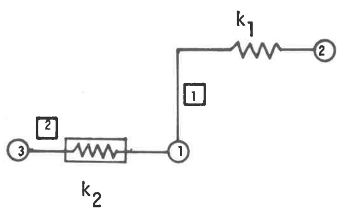

Figure 4 Lumped Element Model of Fuel Storage Module